

PROCYON: 18-MJ, 2- μ s PULSED POWER SYSTEM*

J. H. Goforth, B. G. Anderson, W. E. Anderson, W. L. Atchinson, E. Bartram, J. F. Benage, R. L. Bowers, J. H. Brownell, C. E. Findley, C. M. Fowler, O. F. Garcia, G. J. Heltne, D. H. Herrera, T. J. Herrera, M. Y. Hockaday, G. Idzorek, J. C. King, I. R. Lindemuth, E. A. Lopez, S. P. Marsh, E. C. Martinez, W. Matuska, G. T. Nakafuji, M. C. Thompson, H. Oona, D. L. Peterson, R. E. Reinovsky, M. Rich, J. S. Shlachter, K. D. Sowder, J. L. Stokes, L. J. Tabaka, D. T. Torres, L. R. Veaser, M. L. Yapuncich

Los Alamos National Laboratory
Los Alamos, NM 87545

N. F. Roderick, University of New Mexico
Albuquerque, NM

P. J. Turchi, Ohio State University
Columbus, OH

B. J. Warthen, EG&G
Los Alamos, NM 87544

INTRODUCTION

The Procyon high explosive pulsed power (HEPP) system was designed to drive plasma z-pinch experiments that produce Megajoule soft x-ray pulses when the plasma stagnates on axis. In the proceedings of the Ninth IEEE Pulsed Power Conference,¹ we published results from system development tests. At this time, we have fielded seven tests in which the focus was on either vacuum switching or load physics. Four of the tests concentrated on the performance of a Plasma Flow Switch (PFS) which employed a 1/r mass distribution in the PFS barrel. Of the four tests, two had dummy loads and one had an implosion load. In addition, one of the tests broke down near the vacuum dielectric interface, and the result demonstrated what Procyon could deliver to an 18 nH load. We will summarize PFS results and the 18 nH test which is pertinent to upcoming solid/liquid liner experiments. On our other three tests, we eliminated the PFS switching and powered the z-pinch directly with the HEPP system. From the best of these direct drive tests we obtained 1.5 MJ of radiation in a 250 ns pulse, our best radiation pulse to date. We will also summarize direct drive test results. More details are given in other papers in this conference for both the PFS² and direct drive³ experiments, and an updated analysis of our opening switch performance is also included.⁴ The remainder of this paper describes the parameters and capabilities of our system, and we will use the data from several experiments to provide more precise information than previously available.

APPARATUS

Our 1993 article provided a good description of the Procyon hardware¹ and we will provide only a summary here for completeness. Figure 1 shows a cross section of the Procyon system, Fig. 2 gives a schematic, and Fig. 3 is a photograph of a recent direct drive test near completion.

STORAGE INDUCTOR CURRENT WAVEFORMS

The current waveform from the Procyon storage inductor can be examined in three segments. The first is the period during which the initial magnetic field is injected into the system. Figure 4 shows this segment from a typical test. For comparison, the average value for peak seed current over eight identical tests is 465 kA. The second is illustrated in Fig. 5, which shows both a typical I and di/dt (\dot{I}). This is the wave form produced as the MK-IX

This work was supported by the US Department of Energy.

Report Documentation Page

Form Approved
OMB No. 0704-0188

Public reporting burden for the collection of information is estimated to average 1 hour per response, including the time for reviewing instructions, searching existing data sources, gathering and maintaining the data needed, and completing and reviewing the collection of information. Send comments regarding this burden estimate or any other aspect of this collection of information, including suggestions for reducing this burden, to Washington Headquarters Services, Directorate for Information Operations and Reports, 1215 Jefferson Davis Highway, Suite 1204, Arlington VA 22202-4302. Respondents should be aware that notwithstanding any other provision of law, no person shall be subject to a penalty for failing to comply with a collection of information if it does not display a currently valid OMB control number.

1. REPORT DATE JUL 1995	2. REPORT TYPE N/A	3. DATES COVERED -			
4. TITLE AND SUBTITLE Procyon: 18-Mj, 2-F.Ls Pulsed Power System		5a. CONTRACT NUMBER			
		5b. GRANT NUMBER			
		5c. PROGRAM ELEMENT NUMBER			
6. AUTHOR(S)		5d. PROJECT NUMBER			
		5e. TASK NUMBER			
		5f. WORK UNIT NUMBER			
7. PERFORMING ORGANIZATION NAME(S) AND ADDRESS(ES) Los Alamos National Laboratory Los Alamos, NM 87545		8. PERFORMING ORGANIZATION REPORT NUMBER			
9. SPONSORING/MONITORING AGENCY NAME(S) AND ADDRESS(ES)		10. SPONSOR/MONITOR'S ACRONYM(S)			
		11. SPONSOR/MONITOR'S REPORT NUMBER(S)			
12. DISTRIBUTION/AVAILABILITY STATEMENT Approved for public release, distribution unlimited					
13. SUPPLEMENTARY NOTES See also ADM002371. 2013 IEEE Pulsed Power Conference, Digest of Technical Papers 1976-2013, and Abstracts of the 2013 IEEE International Conference on Plasma Science. Held in San Francisco, CA on 16-21 June 2013. U.S. Government or Federal Purpose Rights License					
14. ABSTRACT					
15. SUBJECT TERMS					
16. SECURITY CLASSIFICATION OF:			17. LIMITATION OF ABSTRACT SAR	18. NUMBER OF PAGES 6	19a. NAME OF RESPONSIBLE PERSON
a. REPORT unclassified	b. ABSTRACT unclassified	c. THIS PAGE unclassified			

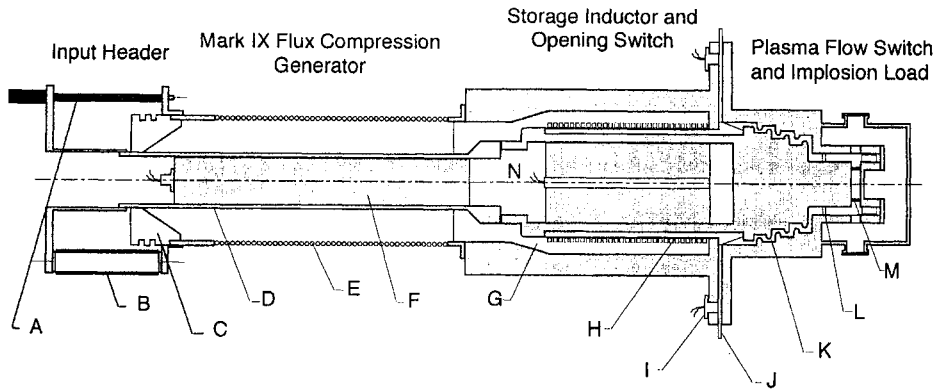


Fig. 1. Procyon assembly with a PFS load. Current flows through A, E, H, and D with insulators C and G and termination resistor B (4Ω). MK-IX explosive, F, shorts out across C, then sweeps flux out of helix (E) into storage inductance, G. Explosive, N, is initiated simultaneously on axis and drives EFF conductor, H, into forming die of G. As EFF resistance rises, closing switches, I, are actuated and current flows through PFS, L, that subsequently switches into implosion load, M.

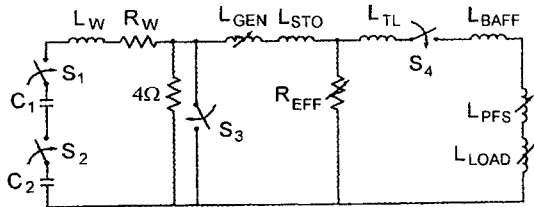


Fig. 2. The schematic shows the initial energy source (C1, C2) not shown in Fig. 1, and the 4Ω resistors (B in Fig. 1) mounted at the MK-IX input. The MK-IX explosive closes the switch, S3, and the remaining configuration is a two loop circuit. We will refer to the two loop equations, and using them to determine the voltage across R_{EFF} . At times of interest to load analysis, L_{GEN} is nearly zero, but L_{STO} is time varying. On direct drive tests, L_{PFS} is constant.

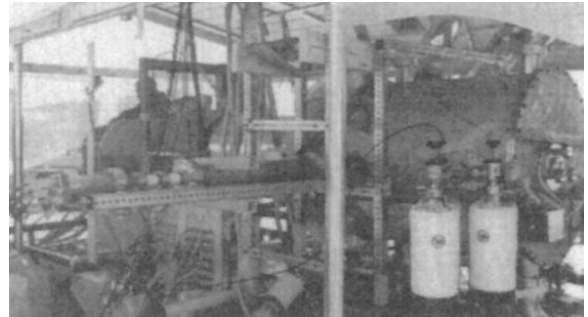


Fig. 3. Recent direct drive test ready to fire. Input header and MK-IX are to the left and vacuum diagnostics chamber to the right.

generator amplifies the initial field and delivers energy to the inductive store. The notches shown in the waveform occur where the MK-IX stator bifurcates. In Fig. 6, another set of waveforms illustrate the last segment. During this interval, the EFF begins to perform flux compression in the circuit (t_1), the closing switch closes (t_2), and current drops in the storage inductor while it increases in the load. Peak transfer occurs at (t_3). Late time features (t_4, t_5) are due to load dynamics.

CIRCUIT ANALYSIS

The current waveforms shown allow us to evaluate many system parameters, but complete analysis of circuit performance requires full knowledge of the storage inductor. As discussed earlier,¹ the exact size of the storage inductor is difficult to determine a priori. Both magnetic and explosive effects have to be accounted for, and geometries are very irregular. In addition, explosive action on the circuit also causes the load circuit transmission lines to

change during a test, and all Procyon experiments have employed dynamic loads. These factors lead to considerable difficulty in determining system values. However, from the data now available, we are able to provide an accurate assessment. For preliminary estimates, we have relied on the ratio of current in the storage inductor initially to that in the circuit when current transfer to the load is complete. For the choice of end points, the system can be viewed in either of two ways. We can evaluate the system by choosing initial values just before EFF dynamics begin (t_1), and the result is a value of ~ 73 nH for the storage inductor. To use this value, however, we must consider that the EFF explosive has reduced the load circuit inductance by 8.5 nH. Alternately, we can take initial points at switch closure time, and view the load transmission line as nearly unchanging. This technique yields approximately 60 nH. Both approaches require estimates of downstream load inductance at the time current equilibrates. Tests with fixed inductance loads downstream from a plasma flow switch have been most useful in our evaluation. Although such analyses now give us accurate end point values, for energy accounting or analysis of opening switch resistance, we must follow the inductances in a continuous way. To make our best approximations, we have estimated values for both storage inductor and load circuit at appropriate times, fitted them together in a reasonable way, and then iterated between the results obtained from upstream and downstream circuit loops. Because this is extremely important in the evaluation of opening switch resistance, details of the process are given in Ref. 4, this conference. The result for the storage inductor is $L_{STO} = 73 \text{ nH} - \int_{t_1}^t (d(L_{STO})/dt)dt$, where t_1 is the time indicated in Figure 6 and $d(L_{STO})/dt$ is a curve given in Ref. 4. Figure 7 shows the energy analysis for a PFS test with an implosion load. To obtain these curves, we have used the function given for L_{STO} , then fabricated L_{LOAD} and $d(L_{LOAD})/dt$ functions that provide good agreement between the two loop equations in the determination of voltage across the EFF (V_{EFF}). Figure 8 shows the degree of agreement achieved, and Fig. 9 shows the L_{LOAD} and

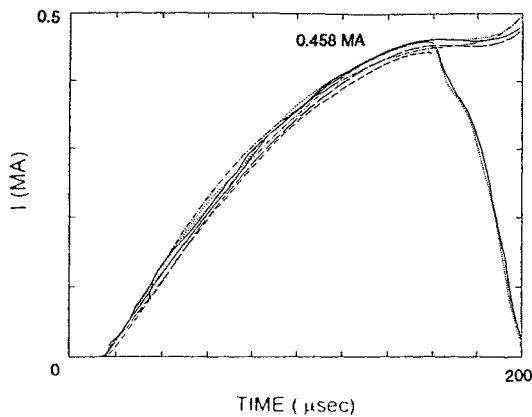


Fig. 4. Initial current from capacitor bank on typical test. The curves that drop at 160 μs are from high sensitivity Faraday probes and yield highest accuracy during this segment.

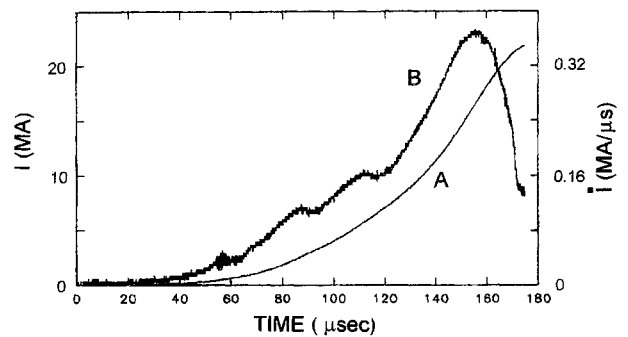


Fig. 5. I (A) and \dot{I} (B) during flux compression phase B is a Rogowski coil output, and A comes either from Faraday probes or a machine integration of B. Notches on B are where MK-IX stator bifurcates.

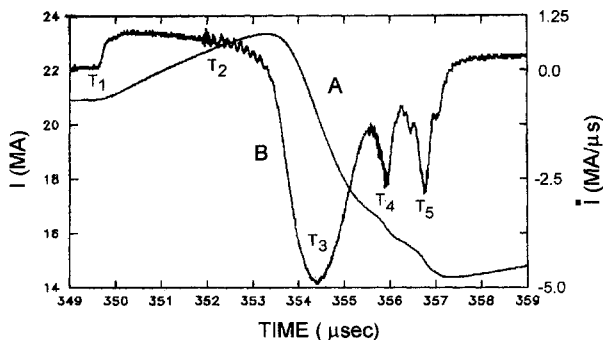


Fig. 6. I (A) and \dot{I} (B) during switching and transfer phase. t_1 is initial motion of EFF, t_2 is closing switch time, t_3 is peak transfer time and t_4 and t_5 are PFS switching and implosion times.

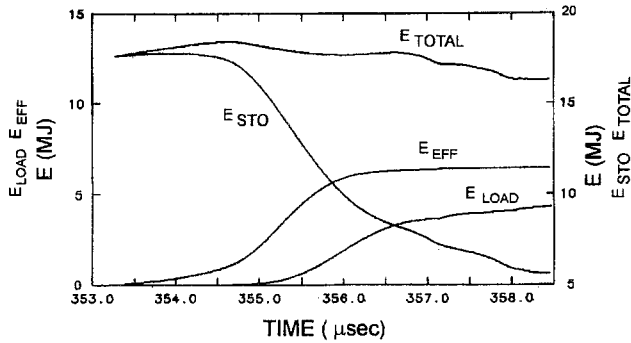


Fig. 7. E_{STO} , E_{LOAD} and E_{EFF} , shown for PFS test with implosion load, are the known magnetic or resistive energy terms in the Procyon circuit. E_{TOT} is the sum, and the step at ~ 358 in E_{TOT} shows that at least 0.9 MJ was available to produce radiation. In addition, explosive effects are adding ~ 0.5 MJ/ μ s to the circuit, and the total available actually exceeds 1 MJ.

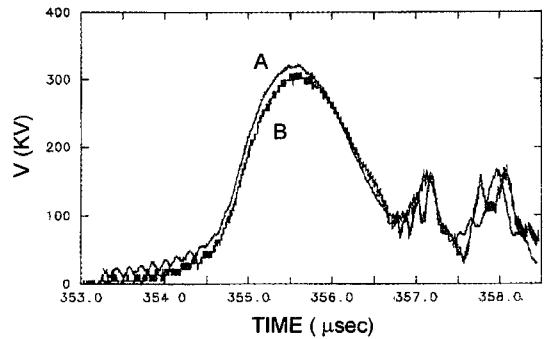


Fig. 8. A is V_{EFF} from the inductive store loop equation and B from the load loop using L and \dot{L} functions shown in Fig. 9 for the load.

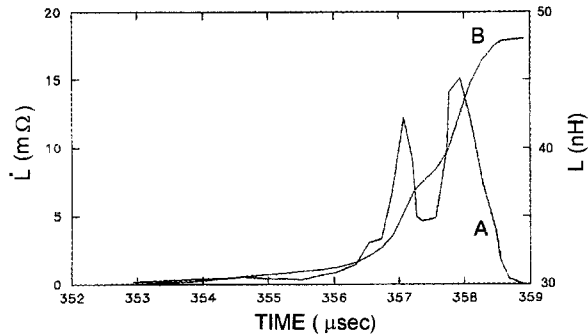


Fig. 9. L_{LOAD} , A, and L_{LOAD} , B, derived for PFS test with implosion load. The two step increases in L are consistent with good PFS switching and a good implosion.

$d(L_{LOAD})/dt$ functions. Figures 7–9 provide a good summary of PFS test results. From Fig. 7 we can determine that ~ 0.9 MJ was available on this experiment to produce radiation. Only ~ 90 KJ were observed, and a broader discussion of this discrepancy is given in Ref. 2. The best explanation is that mass from the PFS absorbs radiation before it gets out. The energy analysis for our best direct drive test is given in Fig. 10–12. In this test, ~ 2.1 MJ were available from the circuit, and 1.5 MJ radiation was observed. 2-D MHD calculations agree well with these data for certain initial perturbations, as is explained in another paper in this conference,⁵ and more data from these tests is given in Ref. 2 and 3.

REPRODUCIBILITY

Our Procyon system has proven to be a very reproducible system, as we illustrate in Figs. 13, and 14. In Fig. 13 we show storage inductor and load currents plotted together for direct drive tests. In Fig. 14 the storage inductor dI/dt is plotted for six tests, and we see that the only significant differences occur as load dynamics begin to dominate. The only adjustments to the data in these figures is to justify the times according to EFF first motion (t_1). Including currents from PFS tests along with those shown in Fig. 13, the storage currents are all within 6%. Figure 14 suggests that the EFF performs quite reproducibly, and further details about the EFF are given in Ref. 4.

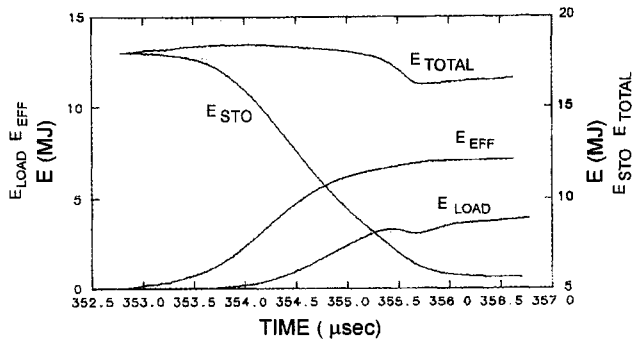


Fig. 10. E_{STO} , E_{LOAD} and E_{EFF} (and their sum, E_{TOT}) curves for our best direct drive test. The step in E_{TOT} at 355.5 shows that ~ 2.1 MJ was available for radiation. 1.5 MJ was observed

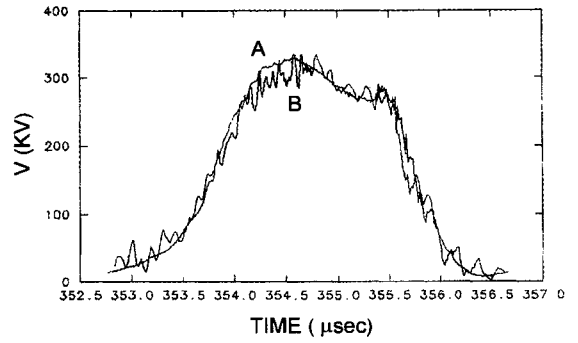


Fig. 11. A is V_{EFF} from inductive store loop and B from the load loop for direct drive test producing 1.5 MJ soft x-rays.

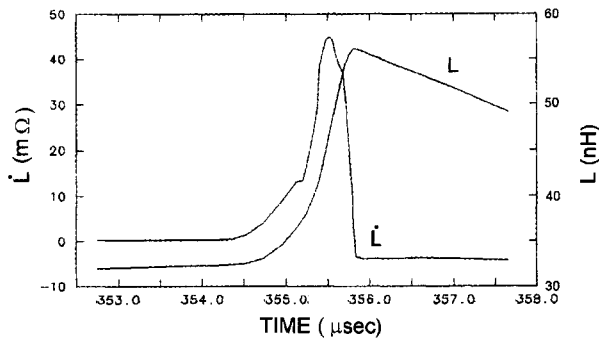


Fig. 12. \dot{L} and L functions derived for load of test producing 1.5 MJ radiation. The 25 nH increase in L is larger than typical.

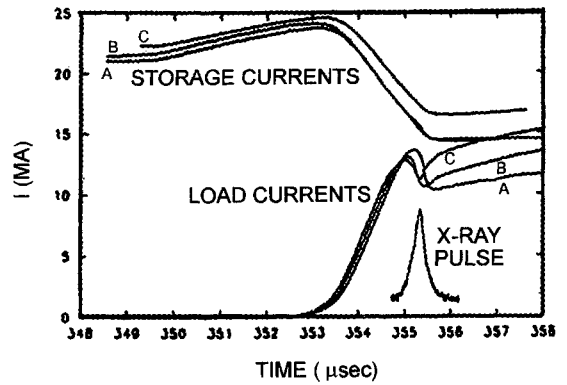


Fig. 13. Store and load currents for three Procyon direct drive tests. The radiation pulse shown goes with test B, our highest yield test.

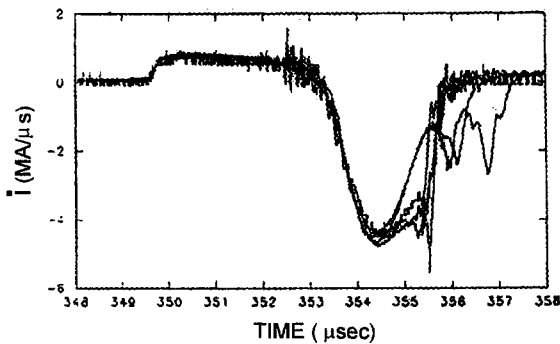


Fig. 14. \dot{I}_{STO} for five Procyon tests showing highly reproducible performance. Differences occur only when load dynamics dominate.

SHORT CIRCUIT RESULTS/LINER DRIVER POSSIBILITIES

On one PFS test, we exceeded the voltage limit of our closing switch and current began to flow prematurely to the load. For ~ 200 ns the voltage on the system rang violently, leading to a failure near the vacuum/dielectric interface. As a result, the load seen by the HEPP system was ~ 18 nH. Since we are now contemplating using Procyon to drive high mass liners that need no radiation baffling, we can build a load of approximately this inductance and this test provides direct insight into what can be expected on such a test. Figure 15 shows the storage and load currents from this test. Peak load dI/dt on this test was $17 \text{ MA}/\mu\text{s}$, and the 10 to 90% current rise time to 20 MA was $1.2 \mu\text{s}$.

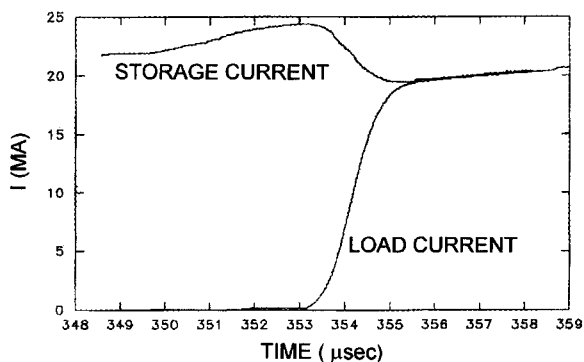


Fig. 15. Store and Load currents for 18 nH load test.

CONCLUSIONS

With the Procyon system we have demonstrated considerable reproducibility in powering vacuum plasma loads, and have shown that we can deliver ~ 20 MA to a solid/liquid liner for high pressure physics studies. Using a PFS, we have achieved good switching to an implosion load, but to date no useful radiation has been observed. On the other hand, our direct drive tests have produced large x-ray fluences. Our best result, to date, is the production of 1.5 MJ of radiation, at a temperature of roughly 60 eV, in a pulse with a full width half maximum of 250 ns. On the other two tests, radiation pulses with the same temperature and 180 and 200 ns wide pulses produced 400 and 600 KJ radiation. On the last of these three tests, we significantly shaped the upstream electrode to enhance an axial jet which was stagnated on a tantalum plate. In addition to measuring a 45 ns wide pulse of ~ 40 KJ from the stagnated jet, we also created a void in the plasma along the shaped electrode. The absence of charge carriers led to a 1.3 MV pulse between the implosion electrodes. In addition to adding an interesting facet to our work, this produced increased high energy radiation, and over 200 KJ of radiation above 300 eV was measured.

ACKNOWLEDGEMENT

The authors wish to recognize the efforts of Samia L. Davis in the preparation of this paper and the paper in Ref. 4 of this conference. In addition we want to thank Mike Christian for his support and encouragement

REFERENCES

1. J. H. Goforth, *et al.* "Review of the Procyon Explosive Pulsed Power System," in Proceedings of the IEEE Pulsed Power Conference, 1993, K. Prestwich and W. Baker, Eds., p. 36.
2. J. H. Benage, *et al.* "Plasma Flow Switch Experiment," this conference.
3. H. Oona, *et al.* "Instabilities in Foil Implosions and the Effect on Radiation Output," this conference.
4. J. H. Goforth, *et al.* "Explosively Formed Fuse Opening Switches for Multi-Megajoule Applications," this conference.
5. D. L. Peterson, *et al.* "Comparison of 2-D Simulation Results with Experimental Results from the PG11-25 Radiation Experiment on the Los Alamos Pegasus II Capacitor Bank," this conference